Title
Formaldehyde over the central Pacific during PEM-Tropics B

Journal
Journal of Geophysical Research, 106(D23)

ISSN
0148-0227

Authors
Heikes, Brian
Snow, Julie
Egli, Peter
et al.

Publication Date
2001-12-16

DOI
10.1029/2001jd900012

JOURNAL OF GEOPHYSICAL RESEARCH, VOL. 106, NO. D23, PAGES 32,717–32,731, DECEMBER 16, 2001

Formaldehyde over the central Pacific during PEM-Tropics B

Brian Heikes,[1] Julie Snow,[1] Peter Egli,[1] Daniel O'Sullivan,[2] James Crawford,[3] Jennifer Olson,[3] Gao Chen,[4] Douglas Davis,[4] Nicola Blake,[5,6] and Donald Blake[5]

Abstract. Formaldehyde, CH_2O, mixing ratios are reported for the central Pacific troposphere from a series of 41 flights, which took place in March-April 1999 as part of the NASA Pacific Exploratory Mission (PEM) -Tropics B mission. Ambient CH_2O was collected in aqueous media and quantified using an enzyme-derivatization fluorescence technique. Primary calibration was performed using aqueous standards and known flow rates. Occasionally, CH_2O gas standard additions to ambient air were performed as a secondary calibration. Analytical blanks were determined by replacing ambient air with pure air. The estimated precision was ±30 pptv and the estimated accuracy was the sum of ±30 parts per trillion by volume (pptv) ±15% of the measured value. Approximately 25% of the observations were less than the instrumental detection limit of 50 pptv, and 85% of these occurred above 6 km. CH_2O mixing ratios decreased with altitude; for example, near the equator the median value in the lowest 2 km was 275 pptv, decreased to 150 pptv by 6 km and was below 100 pptv above 8 km. Between 130 and 170 W and below 1km, a small variation of CH_2O mixing ratio with latitude was noted as near-surface median mixing ratios decreased near the equator (275 pptv) and were greater on either side (375 pptv). A marked decrease in near-surface CH_2O (200 pptv) was noted south of 23°S on two flights. Between 3° and 23°S, median CH_2O mixing ratios were lower in the eastern tropical Pacific than in the western or central Pacific; nominal differences were >100 pptv near the surface to ~100 pptv at midaltitude to ~50 pptv at high altitude. Off the coast of Central America and Mexico, mixing ratios as high as 1200 pptv were observed in plumes that originated to the east over land. CH_2O observations were consistently higher than the results from a point model constrained by other photochemical species and meteorological parameters. Regardless of latitude or longitude, agreement was best at altitudes above 4 km where the difference between measured and modeled CH_2O medians was less than 50 pptv. Below 2 km the model median was approximately 150 pptv less than the measured median.

1. Introduction

The objective of the NASA Pacific Exploratory Mission – Tropics B (PEM-Tropics B) experiment was to further the understanding of tropospheric ozone, the oxidizing power of the atmosphere, and aerosol chemistry and dynamics over the remote Pacific [*Raper et al.*, this issue]. To accomplish this, two instrumented aircraft, the NASA DC-8 and P3-B, were flown from sites in California, Hawaii, Christmas Island, Fiji, Tahiti, Easter Island, and Costa Rica to measure photochemically active gases and aerosols in the tropical and subtropical troposphere away from major anthropogenic pollution sources. The flights occurred in February, March, and April 1999. The PEM-Tropics B mission was a follow-up to the PEM-Tropics A mission at which time, September-October 1996, this same region was found contaminated by the long-range transport of primary pollutants or their by-products from the southern continents and possibly from interhemispheric transport [*Hoell et al.*, 1999]. Formaldehyde is one such photochemically active component that has both anthropogenic and natural origins.

Formaldehyde, CH_2O, is an integral component of atmospheric photochemistry and air pollution. Most atmospheric CH_2O is a secondary photochemical by-product of hydrocarbon oxidation [e.g., *Finlayson-Pitts and Pitts*, 1986], although it is directly emitted into the atmosphere by combustion of fossil fuels and biomass [e.g., *Lee et al.*, 1997]. It is an important step in the atmospheric formation of carbon monoxide, CO, and carbon dioxide, CO_2, and its removal by wet and dry deposition processes can reduce the flow of carbon to these species. The photolysis of CH_2O, its reaction with hydroxyl, HO, or its reaction with nitrogen trioxide at night leads to perhydroxyl radical, HO_2, formation and subsequently, and more importantly, to stronger oxidants like HO and ozone, O_3 [*Logan et al.*, 1981; *Stockwell and Calvert*, 1983]. CH_2O photolysis is also a significant source of molecular hydrogen, H_2. CH_2O may be taken up by atmospheric water where it deposits with precipitation or participates in aquatic reactions with species like dissolved SO_2 or HO [e.g., *Jacob*, 1986; *Chameides and Davis*, 1983].

[1]Center for Atmospheric Chemistry Studies, Graduate School of Oceanography, University of Rhode Island, Narragansett, Rhode Island.
[2]Department of Chemistry, United States Naval Academy, Annapolis, Maryland.
[3]Atmospheric Sciences Division, NASA, Langley Research Center, Hampton, Virginia.
[4]School of Earth and Atmospheric Sciences, Georgia Institute of Technology, Atlanta, Georgia.
[5]Department of Chemistry, University of California, Irvine, California.
[6]Also at Institute for the Study of Earth, Oceans, and Space, University of New Hampshire, Durham, New Hampshire.

Paper number 2001JD900012.
0148-0227/01/2001JD900012$09.00

Typically surfaces like the ocean are thought to be sinks for CH_2O [*Thompson and Zafiriou*, 1983]. However, it may be released to the atmosphere through snow and ice chemistry [*Sumner and Shepson*, 1998], or through the photochemical degradation of dissolved organic matter and biological processes [*Zhou and Mopper*, 1993; *Arlander et al.*, 1990].

The oxidation of methane, CH_4, serves as an example of CH_2O activity in atmospheric photochemistry. CH_4 oxidation is thought to be the dominant hydrocarbon oxidation pathway in the photochemistry of the remote troposphere and to be the predominant parent hydrocarbon for CH_2O. CH_4 reacts with OH and subsequently oxygen to make methylperoxy radicals:

$$CH_4 + OH \rightarrow CH_3 + H_2O \quad (1a)$$

which is rapidly followed by

$$CH_3 + O_2 \rightarrow CH_3OO. \quad (1b)$$

Depending upon the relative concentration of nitric oxide, NO, and HO_2, methylperoxy radicals will yield CH_2O and nitrogen dioxide, NO_2, or methylhydroperoxide, CH_3OOH:

$$CH_3OO + NO \rightarrow CH_2O + NO_2 \quad (2)$$

or

$$CH_3OO + HO_2 \rightarrow CH_3OOH + O_2. \quad (3)$$

Unless removed heterogeneously, CH_3OOH is ultimately oxidized to CH_2O by photolysis or reaction with HO:

$$CH_3OOH + light \rightarrow CH_3O + HO \quad (4a)$$

which is rapidly followed by

$$CH_3O + O_2 \rightarrow CH_2O + HO_2 \quad (4b)$$

or

$$CH_3OOH + HO \rightarrow CH_2OOH + H_2O \quad (5a)$$

which is rapidly followed by

$$CH_2OOH \rightarrow CH_2O + OH. \quad (5b)$$

Like CH_3OOH, the resulting CH_2O, which is not removed heterogeneously, undergoes photolysis or reaction with HO to produce CO, H_2, and HO_2:

$$CH_2O + light \rightarrow CO + H_2 \quad (6)$$

or

$$CH_2O + light \rightarrow CHO + H \quad (7)$$

and

$$CH_2O + HO \rightarrow CHO + H_2O, \quad (8)$$

where the products of (7) and (8) rapidly react with oxygen:

$$CHO + O_2 \rightarrow CO + HO_2 \quad (9)$$

and

$$H + O_2 \rightarrow HO_2. \quad (10)$$

In the presence of oxygen, CO reacts with HO yielding CO_2 and HO_2:

$$CO + HO \rightarrow HOCO + O_2 \rightarrow CO_2 + HO_2.$$

Lastly, depending upon the relative concentrations of NO, O_3, and HO_2, the HO_2 yields NO_2, HO, hydrogen peroxide (H_2O_2), and oxygen:

$$NO + HO_2 \rightarrow NO_2 + HO \quad (11)$$

$$HO_2 + HO_2 \rightarrow H_2O_2 + O_2 \quad (12)$$

or

$$HO_2 + O_3 \rightarrow HO + 2O_2.$$

CH_2O has a role in HO_x chemistry and in ozone production as a source of HO_2 and hence NO_2. Clearly, CH_2O measurements together with observations of other photochemically active species, for example, NO, NO_2, H_2O_2, CH_3OOH, HO, HO_2, CO, are powerful tools in testing our understanding of ozone production, hydrocarbon oxidation and, in general, the oxidizing power of the atmosphere represented by O_3 and HO [*Raper et al.*, this issue].

Prior airborne observations of CH_2O in the remote atmosphere are at various levels of agreement with photochemical models. Recently, *Arlander et al.*, [1995], using a cartridge collection and DNPH derivatization technique in the Tropospheric Ozone second airborne campaign (TROPOZ II) (January-February 1991, a circumnavigation of North Atlantic and South America), showed CH_2O concentrations larger than those expected based upon CH_4 photochemistry alone. They noted much better agreement when the measurements were stratified by latitude and altitude and compared with a model that incorporated three-dimensional transport. In the Subsonic Assessment Ozone and Nitrogen Oxide Experiment (SONEX) (October-November 1998, covering the North Atlantic flight corridor), CH_2O measurements, using the aqueous collection and enzyme derivatization method used here and described below, showed a similar variance with a photochemical point model [*Jaegle et al.*, 2000], and Jaegle et al. suggested and showed that inclusion of a heterogeneous source improved the agreement. *Singh et al.* [2000], using the same measurements and a three-dimensional photochemical transport model, found much closer agreement when comparing latitude-altitude stratified and averaged data with their model simulations. A. Fried et al. (manuscript in preparation, 2001) reported measurements of CH_2O from the North Atlantic Regional Experiment (NARE) 1997 (April 1997 along the northeast coast of the United States and western North Atlantic). Their observations were made using two techniques, a tunable diode laser absorption spectroscopy method and an aqueous collection and DNPH derivatization method, and these independent observations have been shown to be greater than those predicted using a photochemical point model (G. Frost et al., manuscript in preparation, 2001). In contrast, Heikes et al. [1996b] and *Jacob et al.* [1996] showed Transport and Atmospheric Chemistry Near the Equator–Atlantic (TRACE-A) (South Atlantic Basin, October-November 1992), marine boundary layer measurements were significantly lower than models would suggest but that measurements and model results were in agreement in the more remote free troposphere away from continental emissions. In this paper it will be shown that the near-surface CH_2O measurements from PEM-Tropics B are also larger than those expected based upon point photochemical models [*Olson et al.*, this issue; *Ravetta et al.*, this issue; J.M. Rodriguez et al., manuscript in preparation, 2001]. However when stratified and averaged, the observations were consistent with predictions from higher-dimensional photochemical models [*Wang et al.*, this issue; *Singh et al.*, 2001].

Implicit in the model-measurement comparisons is the noteworthy improvements with altitude-latitude stratification and averaging and with the inclusion of transport in the models. It should be pointed out that the measurement methods employed in TROPOZ, NARE, SONEX, and PEM-Tropics B were all operating at or within a factor of 10 of their reported detection limits. Averaging should remove random instrumental effects, but there is still the general offset between measurements and point model results to be explained. CH_2O has a lifetime of only a few hours under the photochemical conditions found in the tropics and subtropics during PEM-Tropics B. Hence the inclusion of horizontal transport is not expected to improve the comparison of measured and modeled CH_2O within a region several days removed from significant emissions or synoptic-scale perturbations. However, it does suggest 1-100 km scale meteorological processes such as convective vertical motion associated with individual clouds or organized mesoscale convective complexes could effect CH_2O concentrations; such an effect has been suggested by models and measurements of CH_3OOH and odd-hydrogen radicals near and downwind of convective systems [*Prather and Jacob*, 1997; *Cohan et al.*, 1999; *Wennberg et al.*, 1998; *Jaegle et al.*, 1997].

A similar level of disagreement exists between surface CH_2O measurements and point models of the marine boundary layer. *Ayers et al.*, [1997] showed observations at Cape Grim, Tasmania (November-December, 1993), were approximately 50% higher than a point model would predict, and they suggested reaction (3) above may have an alternate channel yielding CH_2O, H_2O, and O_2 under low NO_x and high water vapor conditions. This bypasses the formation of CH_3OOH and yields CH_2O directly. *Weller et al.* [2000] showed shipboard observations in the South Atlantic from the Albatross campaign (October-November, 1996), which were a factor of 3 greater than point model results. However, three episodes of relatively clean air with low CH_2O in their data set and the observations and model results reported by *Junkermann and Stockwell* [1999] for the same region during October-November, 1994, gave agreement within model-measurement uncertainty. Both Junkermann and Stockwell and Weller et al. dismissed the alternate channel hypothesis.

In this paper we describe the CH_2O method employed in PEM-Tropics B and summarize CH_2O distributions over the central Pacific during PEM-Tropics B. Other papers in this special issue will address CH_2O's concentration by air mass type [e.g., *Avery et al.*, this issue; *Browell et al.*, this issue; Fuelberg et al., manuscript in preparation, 2001; J.Snow et al., unpublished manuscript, 2001], its roles in ozone production and oxidation capacity [e.g., *Olson et al.*, this issue; *Wang et al.*, this issue; J.M. Rodriquez et al., manuscript in preparation, 2001], in HO and HO_2 chemistry [e.g., *Ravetta et al.*, this issue; J.M. Rodriquez et al., manuscript in preparation, 2001], and its role, as one of many oxygenated carbon compounds, in atmospheric carbon chemistry [*Singh et al.*, 2001].

2. Methodology

Ambient gaseous CH_2O was quantified using the aqueous collection and enzyme-fluorescence detection method of *Lazrus et al.* [1988] with minor modifications [Heikes et al., 1996a,b]. In this method, CH_2O vapor is first collected in concurrent-flow coil collectors using ultrapure water acidified with hydrochloric acid (HCl; pH=3). The collection solution effluent from the coil is first buffered to pH 8 and then combined with formaldehyde dehydrogenase enzyme and nicotinamide adenine dinucleotide (oxidized) to yield a fluorescence product, nicotinamide adenine dinucleotide (reduced). The amount of fluorescence product is proportional to the amount of CH_2O collected. Earlier intercomparison studies [*Kleindienst et al.*, 1988; *Lawson et al.*, 1990; *Heikes et al.*, 1996a; *Gilpin et al.*, 1997] have shown the method to be comparable to other techniques and virtually free of artifacts and interferences under synthetic ambient concentrations ranging from a few hundred pptv to over 10,000 pptv. The collection efficiency of the coil collectors can vary as the collection of CH_2O is kinetically controlled [*Lazrus et al.*, 1988; *Lee and Zhou*, 1993; *Gilpin et al.*, 1997], and thus it must be determined over the full range of environmental sampling conditions. It should be noted that on Christmas Island, HCl was unavailable to acidify the collection water used on the P3-B aircraft. Nitric acid and sulfuric acid were available and tested as alternative acidifying agents. Nitric acid at 10^{-3} *M*, or an impurity in the nitric acid, was found to cause a nearly complete loss of CH_2O signal. This was the case for aqueous CH_2O standards, gas-phase CH_2O standards, and ambient air. Sulfuric acid was found to be a suitable substitute, and CH_2O measurements reported from the P3-B at Christmas Island were made using sulfuric acid in the collection water.

A dual collector-fluorometer system was implemented on both the DC-8 and P3-B aircraft in PEM-Tropics B. Each system used a 20-min cycle alternating between a 10-min collection/measurement period and a 10-min pure-air blank period. The time response characteristics of the collection coil and aqueous reagent mixing necessitated the removal of 5 min of signal between blank and measurement periods. The two systems alternated between measurement and blank mode. This results in 5 min of usable measurements every 10 min.

Figure 1 shows a schematic of the airflow plumbing on the DC-8. The P3-B system was identical except the gas-phase CH_2O standards generator was not employed due to weight and space restrictions. On each aircraft, ambient air was drawn into the aircraft using a combination of a diffuser inlet, electro-mechanical diaphragm pump, and venturi exhaust pump. The combination of the diffuser and venturi was adequate to permit sampling without the pump below 9 km. However, the risk of electrical transients upon restarting the pump when sampling above 9 km was considered too great, and the pump was left on at all times. The external inlet, shared between the peroxide system (D.W. O'Sullivan et al., unpublished manuscript, 2001) and the formaldehyde system, was heated to 35°C. Analytical blanks were determined by introducing pure air (Scott Marrin, Riverside, California) into the sample manifold just prior to one of the aqueous collection coils. The other coil was then used to collect ambient samples. A "four-port" valve was fabricated and used to alternately switch sample air or pure air between each of the collection coils. Mass flow controllers were used to regulate gas flow through the collection coils (nominally 1.5 standard liters per minute, sLpm), the pure air blank flow (nominally 2.5 sLpm), and the inlet and pure air excess flow (nominally 2 sLpm). A peristaltic pump with tygon tubes was used to control the addition rate of collection solution (nominally 0.0004 Lpm; calibrated using a stopwatch and

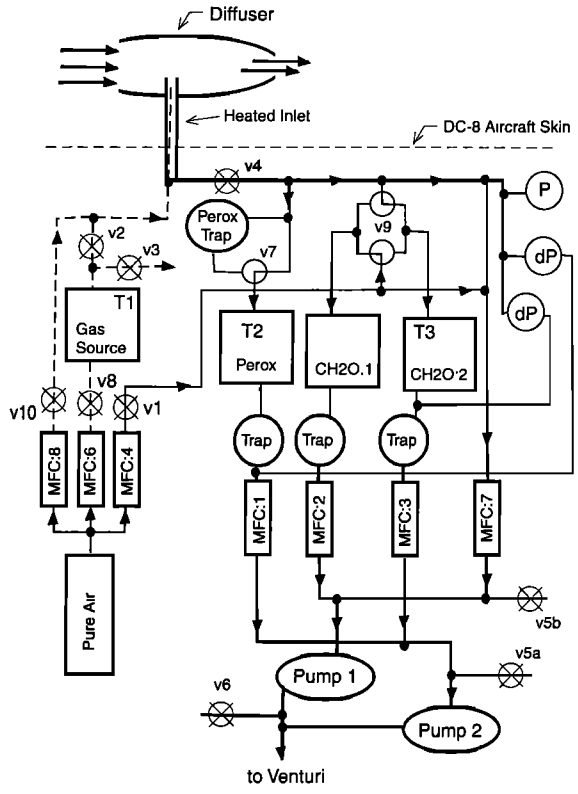

Figure 1. Schematic diagram of DC-8 inlet and gas sampling plumbing especially CH_2O sample plumbing. Thin lines indicate ¼ inch PFA Teflon tubing, and thick lines indicate 3/8 inch PFA Teflon tubing. Thin dashed line is an 1/8 inch PFA Teflon tube catheter used to introduce pure air or standard gases approximately 3 inches in from the tip of the inlet. "T" indicates thermister location, "P" is an absolute pressure transducer and "dP" is differential pressure transducers. V9a and V9b are 2 three-way Teflon valves that comprised the ambient – pure-air switching valve for CH_2O blank determination. MFC denotes mass flow controllers. Diffuser inlet is designed to boost inlet pressure without sampling large particles. Venturi exhaust is used to provide exhaust vacuum to boost pumping speed at high altitude. The diffuser venturi combination permitted ambient sampling without the use of electro-mechanical pumps below 9 km.

precision balance). Mass flow controllers were calibrated using a volumetric flow calibration system corrected to a standard reference temperature and pressure of 273.15°K and 1013.25 hPa, respectively. Coil collection-solution flow rates were determined using the input flow rate to the coil after correction for evaporation using monitored temperature, pressure, and volume flow rate. The coil effectively saturates the airstream at the temperature of the collection solution.

Primary calibration was performed using aqueous standards and known gas and aqueous flow rates. These calibrations and possible inlet artifacts and interferences were examined on the DC-8 by occasional gas phase standard additions of CH_2O to ambient air, nominally a 1000 ppt addition to ambient mixing ratios. The standard addition process requires 30 min to complete and steady ambient CH_2O mixing ratios. Hence it could not be used as the primary calibration method on a routine basis. A 1/8 inch PFA Teflon tube was run as a catheter inside the inlet tube to introduce standard gases within 3 inches of the inlet tip. Within the constraints of flight tracks flown, natural variability of CH_2O in the ambient air, timing cycle, and precision, the gas-phase standard additions were all within 30% of the expected value based upon the aqueous calibrations and within instrumental accuracy. The detection limit of the instrument is estimated to be 50 pptv based upon 3 times the standard deviation of the blanks. The accuracy of the measurement is estimated to be the sum of ±30 pptv ±15% of the value. The ±15% is based upon a propagation of errors (aqueous calibration, ±5%, gas flow rate, ±5%, aqueous flow rate, ±5%, and collection efficiency ±13%), with uncertainty in collection efficiency contributing the largest portion.

A photochemical point model [*Crawford et al.*, 1999; *Olson et al.*, this issue] was used to predict CH_2O and to help analyze observed CH_2O. The model was forced by the suite of photochemically important constituents measured onboard the two aircraft. Principle species forcing the model include but are not limited by NO, CO, CH_4, low molecular weight hydrocarbons($<C_3$), H_2O, O_3, and the state variables: spectral actinic flux, temperature, and pressure. Measured H_2O_2 and CH_3OOH, as well as CH_2O, were not used to force the model in the CH_2O comparison simulations. The instantaneous steady state model results are presented for comparison with the observations owing to CH_2O lifetime being on the order of a couple of hours. Our findings did not change appreciably when diel-averaged CH_2O model results were used.

The chemical observations and model results reported here are taken from a 1-min merge product. The merge process has been described elsewhere [e.g., *Heikes et al.*, 1996b], and is not repeated here. In the case of CH_2O the observation and merge periods are on a whole min basis such that observations and 1-min merge product averages are coincident for all practical purposes. The model used the 1-min merge product concentrations as input, and its results are on the same timeframe. Therefore we have used 1-min merge product's CH_2O data as those observed.

3. Results

The geographical location of all CH_2O measurements is shown for both aircraft in Figure 2a. The thin line shows the P3-B and DC-8, flight tracks, and the thicker portion denotes where CH_2O was sampled. All 5633 1-min merge product CH_2O observations are indicated. A longitude-altitude cross section (Figure 2b; 3015 observations shown) and a latitude-altitude cross section (Figure 2c; 3709 observations shown) were defined based upon flight geography and sample locations. The longitude–altitude cross section is restricted to latitudes between 23° and 3°S, and the latitude-altitude cross section is restricted to longitudes between 130° and 170°W. Figure 2a also shows several geographical subsections separated by the heavy dashed lines and labeled A, B, C, D, E, and F, 1, 2 and 3. These subsections are indicated in Figure 2b (1-3) and in Figure 2c (A-F), also. Observations shown in subsections B and C are the same as those in subsection 2. The nominal latitude of a diffuse Intertropical Convergence Zone (ITCZ) was 7°N [*Fuelberg et al.*, this issue], and the ITCZ and this latitude serve to anchor our latitudinal 10° stratification boundaries: 23°S, 13°S, 3°S, 7°N, and 17°N. The following altitudes; 0, 1, 2, 4, 6, 8, 10, and 12 km, were used to segregate the data into seven altitude zones, as well. There were only a few observations above 12 km, and these have been ignored. The labels d21 and d22 on

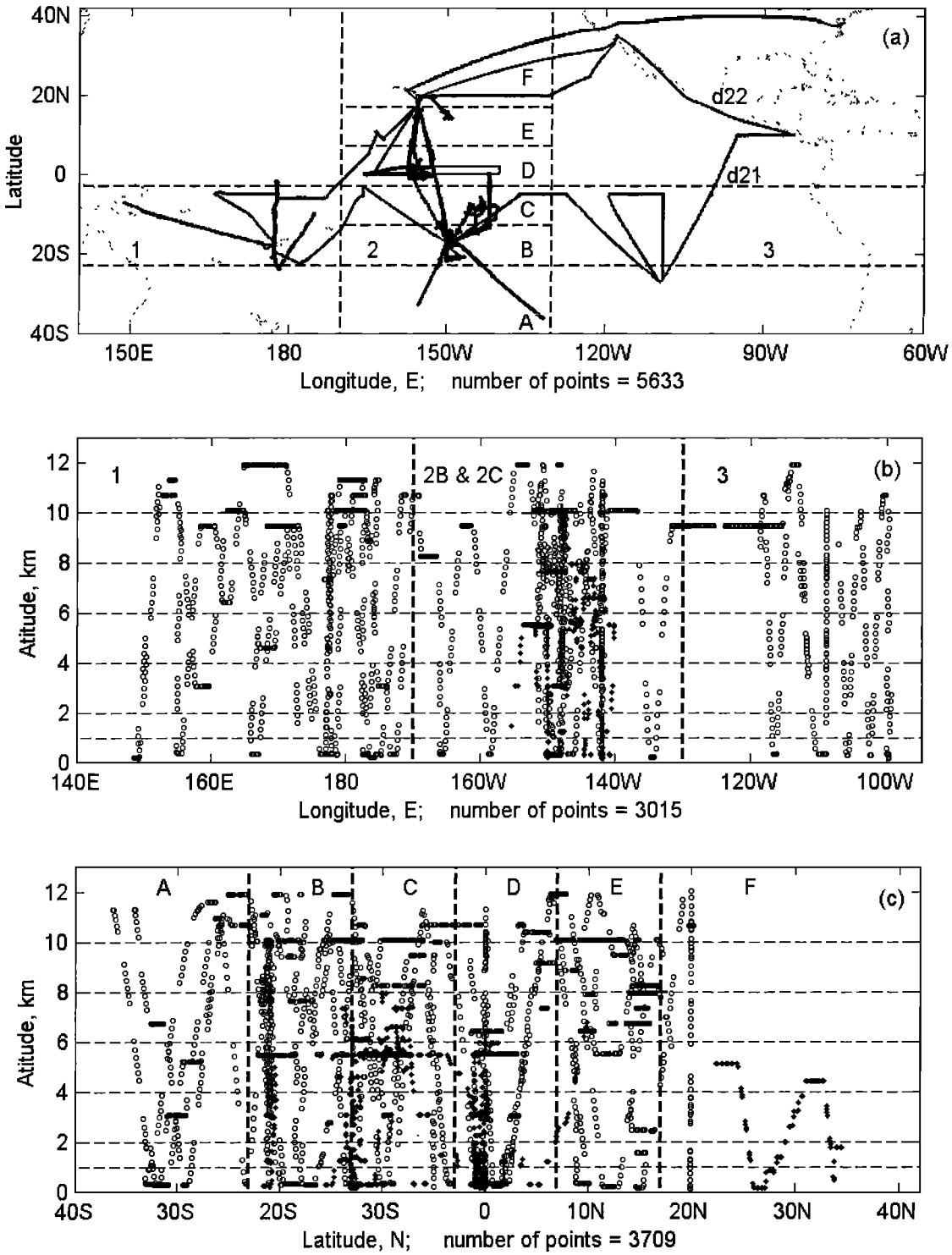

Figure 2. (a) Geographical location of CH_2O samples, thick line/symbol; and DC-8 and P3-B flight tracks, thin lines. Thick dashed lines and labels 1-3 and A-F designate subdomains used to stratify data for longitudinal and latitudinal cross sections. (b) Altitude-longitude cross section of CH_2O sample locations between 3° and 23°S. Symbol spacing during ascent or descent illustrates instrument 10-min mode and 1-min sample periods. Vertical thick dashed lines and labels 1, 2B, 2C, and 3 denote longitudinal subdomains for data stratification presented in Figure 6. Horizontal thin dashed lines denote vertical layers used for data stratification by altitude. A total of 3015 data locations are shown. (c) Altitude-latitude cross section of CH_2O between 130° and 170°W. Thick dashed line and labels A-F denote latitudinal subdomains for data stratification presented in Figure 5. Horizontal thin lines are the same as in Figure 2b. A total of 3709 data locations are shown.

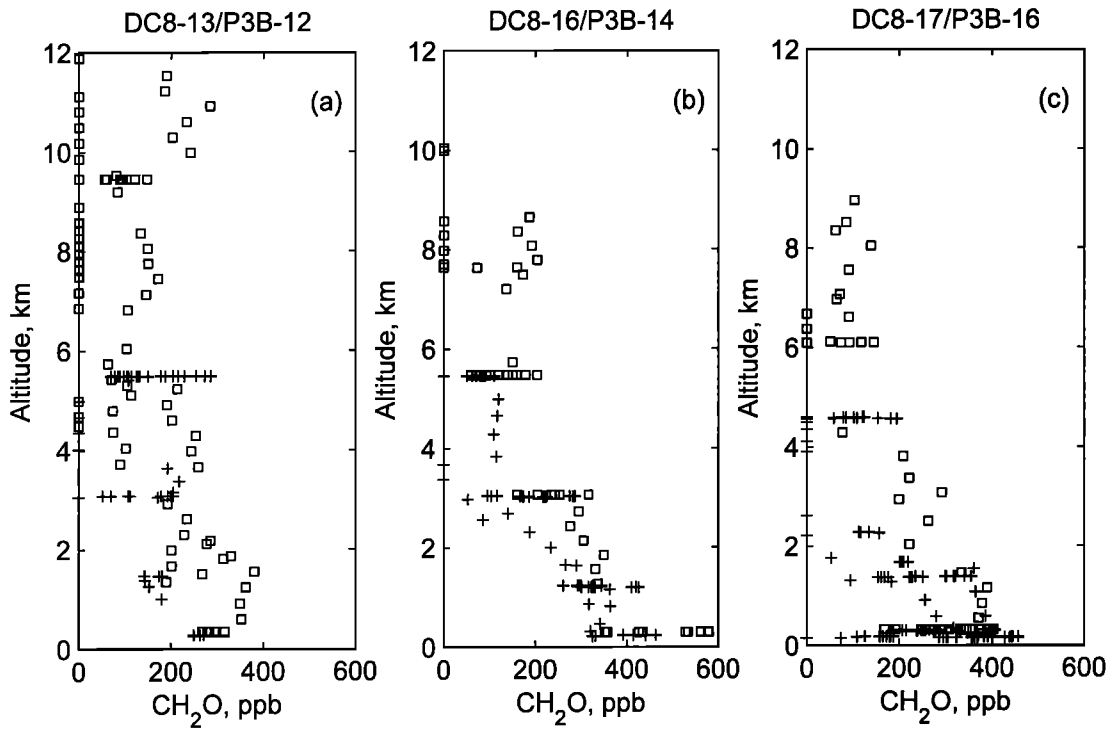

Figure 3. Vertical profiles of CH_2O from the P3-B (pluses) and DC-8 (open squares). (a) DC-8 flight 13, Fiji to Tahiti, and P3-B flight 12, Christmas Island to Tahiti. Data shown are east of 165°W and south of 1°S. (b) Data from sections of DC-8 flight 16 and P3-B flight 14 south of 20°S and east of 148.5°W, Tahiti local flights. (c) Data south of 12°S and east of 143°W from DC-8 flight 17 and P3-B flight 16, Tahiti local flights.

Figure 2a indicate approximate locations of CH_2O plumes observed below 5 km near Costa Rica and southern Mexico during DC-8 flights 21 and 22, respectively, and which are discussed below.

The CH_2O measurements from the DC-8 and P3-B are pooled together. Identical analytical methods were used on both aircraft. Indications are that the two systems performed similarly and systematic differences are unimportant; however, without direct plane-to-plane intercomparison this is difficult to prove. There are three pairs of DC-8 and P3-B flights in which both CH_2O instruments were working, and it may be concluded each aircraft was sufficiently close to the other in time and space such that they sampled the same chemical air mass. CH_2O data from segments of these flight pairs are shown in Figure 3. Sections of DC-8 flight 13 (Fiji to Tahiti) and P3-B flight 12 (Christmas Island to Tahiti) east of 165°W and south of 1°S are shown in Figure 3a. These measurements were taken in and around thunderstorms. Multiple ascents and descents several degrees of arc apart and several hours apart are compressed onto a single vertical profile. There is overlap in the data range observed between aircraft within constant altitude regions (e.g., 1.5, 3, 5.5 km), although individual profiles appear distinct. Figure 3b shows data from sections of DC-8 flight 16 and P3-B flight 14 south of 20°S and east of 148.5°W. These data represent the flight pair closest in time and geographic location. They also indicate the closest correspondence in mixing ratios at a given altitude. CH_2O mixing ratios south of 12°S and east of 143°W from DC-8 flight 17 and P3-B flight 16 are shown in figure 3c. Again, range overlap is noted at the common altitudes of 1 3 and 5.5 km. Multiple species (e.g., O_3, H_2O, C_2H_6, DMS, CH_3I) were compared for these same flight portions, and while not shown here, these data indicate small variability in the air mass sampled by the two aircraft on these respective days.

A geographically defined comparison zone was made, and data distributions from the two aircraft were examined to further test for bias between the two aircraft instrument systems. CH_2O histograms from seven altitude bins; 0-1, 1-2, 2-4, 4-6, 6-8, 8-10, and 10-12 km, bounded by 3°-23°S and 130°-170°W are shown on Figure 4. The comparison zone thus defined contained measurements from seven DC-8 flights and six P3-B flights made on 10 different days. From left to right each column of histograms shows DC-8 data only, P3-B data only, pooled data, statistically sampled model results, and model results, respectively. In a column of histograms the bottommost is for 0-1 km, and the topmost is for 10-12 km. Each histogram uses a cell width of 50 pptv starting at 0. The first cell in a histogram, 0-50 pptv, indicates the number or percentage of observations within that stratum below the level of detection (LOD) limit. The last cell, 550-600 pptv, indicates the number or percentage of observations greater than 550 pptv. The downward pointing triangle shows the median CH_2O mixing ratio for each stratum. In the two leftmost columns of histograms the height of an individual cell bar shows the number of observations within a cell in each stratum. The cell bar height indicates the percent of occurrence in the three rightmost columns of histograms. The practical ceiling of the P3-B was just above 8 km, and there are few observations between 8-10 km and none above 10 km from the P3-B. From Figure 4 it can be seen that the mode, median, and distribution of CH_2O observed by each aircraft

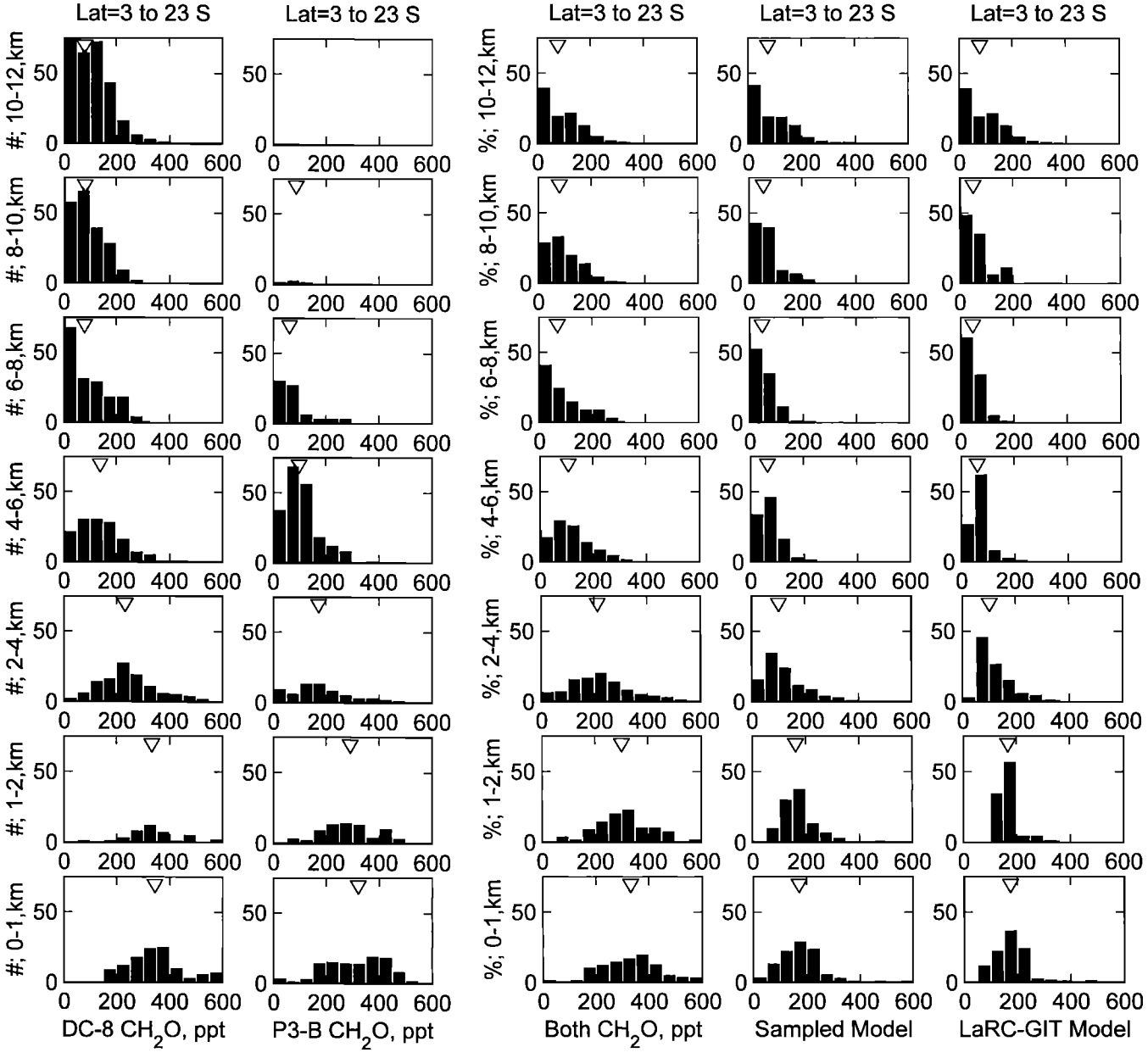

Figure 4. CH_2O histograms for the DC-8 (leftmost column of histograms labeled DC-8) and the P3-B (column of histograms second from left labeled P3-B) for latitudes 3°-23°S, longitudes 130°-170°W, and seven altitude zones. Each histogram cell width is 50 pptv which corresponds to the instrument level of detection. The leftmost histogram cells show the number or percent of data below the detection limit for each stratum, and the rightmost histogram cells show the number or percent of observations greater than 550 pptv within each stratum. Individual histogram X axis labels give CH_2O mixing ratio. Individual Y axis labels indicate altitude range of stratum, the "pound sign" indicates number of samples within a histogram cell, and the "percent symbol" indicates percent of occurrence within a histogram cell for each stratum. The downward pointing triangles indicate the CH_2O median value for each stratum. Altitude bins are 0-1, 1-2, 2-4, 4-6, 6-8, 8-10, and 10-12 km. The middle column of histograms labeled "Both" is for the DC-8 and P3-B pooled data. The column of histograms second from the right labeled "Sampled Model" is for model results sampled using a statistical instrument with precision and accuracy equal to the real CH_2O instrumentation. The rightmost column of histograms labeled "LaRC-GIT" is data from the photochemical point model.

was nearly identical. This together with the three flight pairs shown in Figure 3 gives us confidence in pooling the data from the two aircraft for subsequent discussion of CH_2O. The centermost column of histograms in Figure 4 shows the percent of occurrence for the combined observational set.

Model results are shown on Figure 4 for the same geographically defined DC-8 and P3-B comparison zone defined above, 3°-23°S and 130°-170°W. They are the rightmost column of histograms labeled "LaRC-GIT Model." The histograms are defined as above and the downward

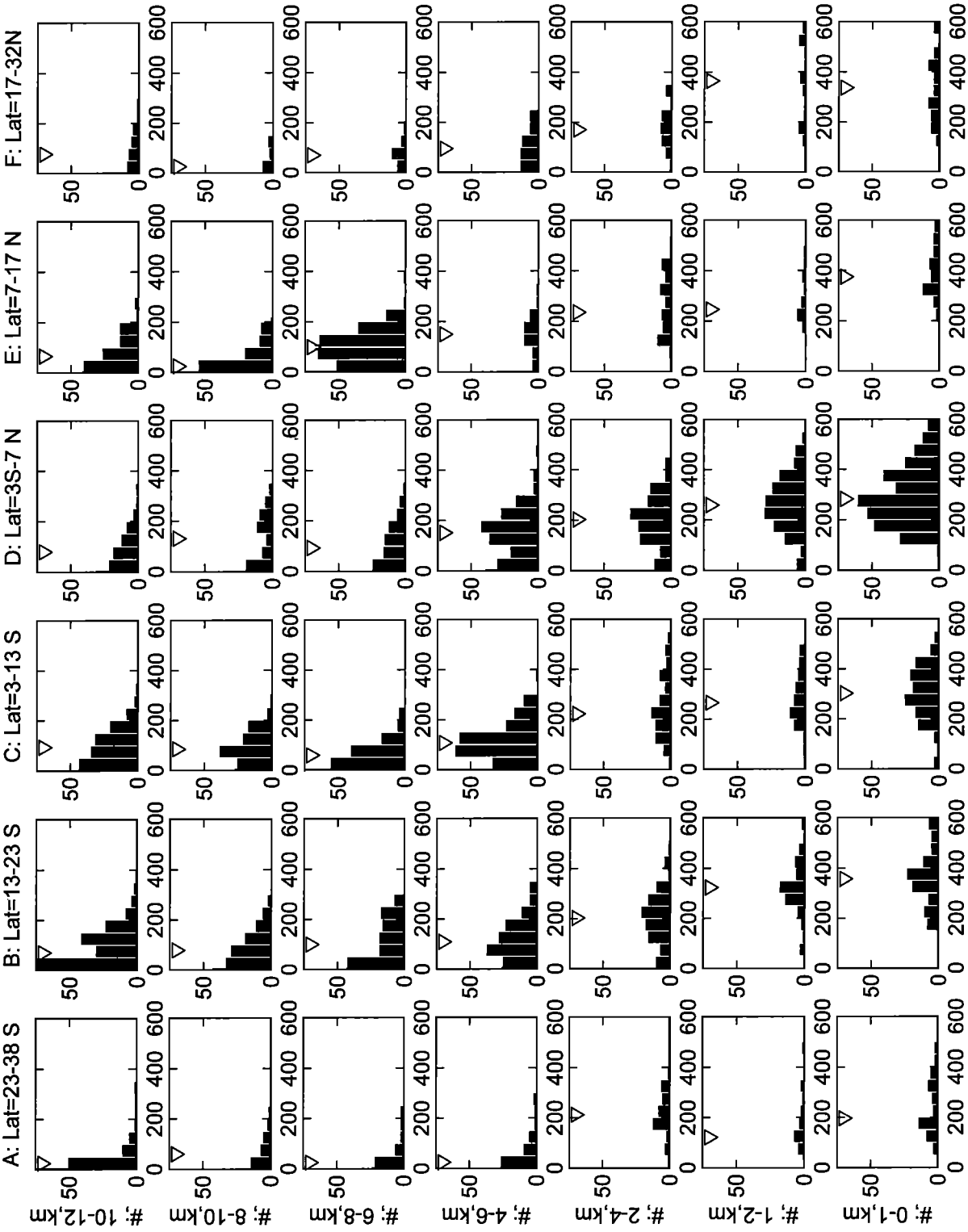

Figure 5. North-south transect across the central Pacific between 130° and 170°W for pooled DC-8 and P3- B data sets. Latitude zones 38°-23°S, 23°-13°S, 13°-3°S, 3°S-7°N, 7°-17°N, and 17°-32°N are indicated across top of figure and go from left to right. Zone label is referenced to Figure 2. Histograms are defined as in Figure 4 for the different altitude and latitude zones. Median values for each stratum are indicated by the downward pointing triangle.

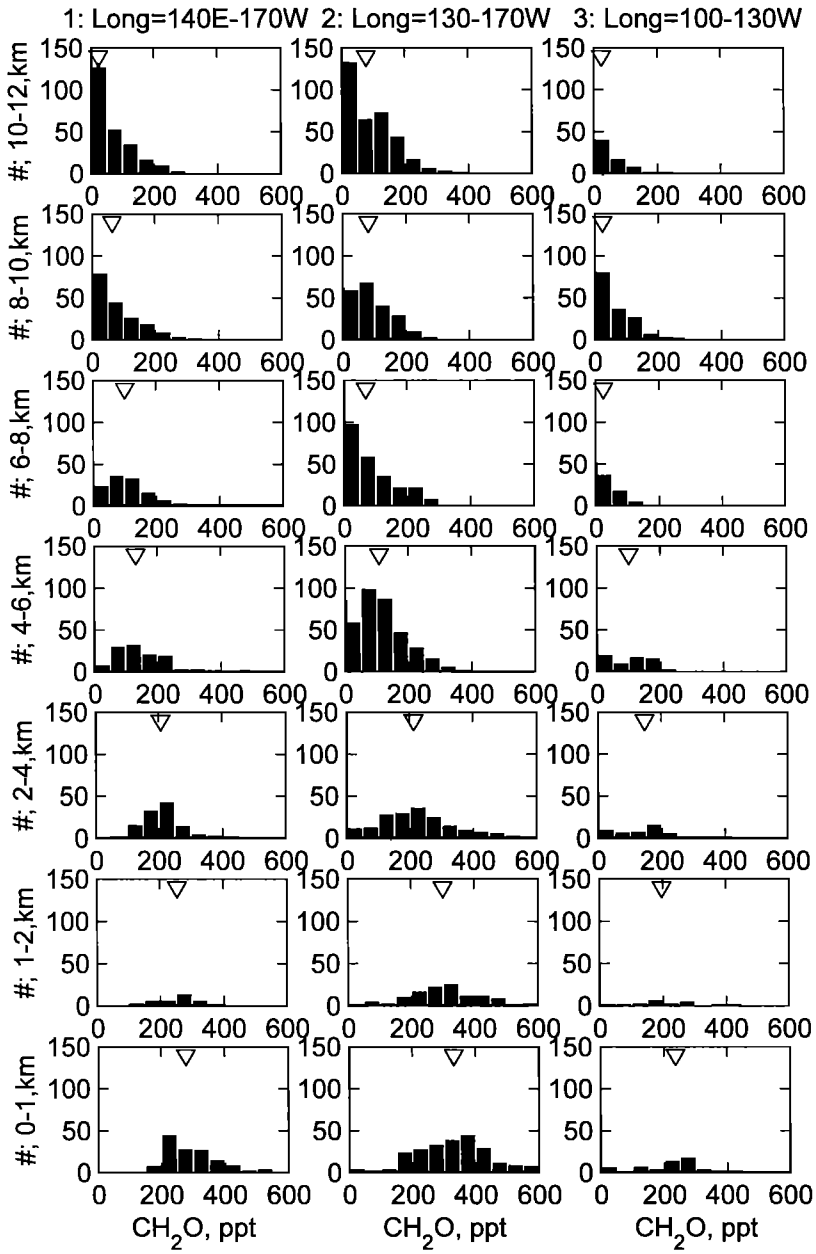

Figure 6. Same as Figure 5 except for a west-east transect between 3° and 23°S. Longitude zones 140°E-170°W, 130°-170°W and 100°-130°W are indicated across the top and go from left to right. Histograms are defined as in Figure 4 for the different altitude and longitude zones. Median values for each stratum are indicated by the downward pointing triangle.

pointing triangles indicate the median CH_2O model result. Owing to the large difference in the numbers of observations verses model results, the histogram cell heights show percent of occurrence rather than number of events within each cell width. This is the case for the center and middle-right columns of histograms, too. The center column labeled "Both" presents the DC-8 and P3-B pooled data set. It is noted on Figure 4 and on Figures 5 and 6 below that the percentage of observations less than the LOD increases with altitude. Comparisons of model-measurement averages are increasingly tenuous with increasing altitude because of the increasing frequency of occurrence of LOD values. Hence it is no longer possible to directly calculate a meaningful measurement average. Consequently, we argue it is more meaningful to compare medians and distribution parameters such as inner and outer quartiles. Above 4 km the model medians and pooled medians are in agreement to within 50 pptv, and above 8 km the model result median is approximately 40 pptv, whereas the measured median is approximately 55 pptv. The model result median CH_2O is approximately 150 pptv less than the observed median in the 0-1 and 1-2 km layers. Figure 4. clearly shows the model results were more narrowly distributed than the observed mixing ratios.

One explanation for the difference in distribution width between the observed and model result data is random measurement error when an instrument is operating close to its level of quantification, as was the case for CH_2O in PEM-

Tropics B. To assess the significance of random measurement error, a statistical CH_2O "instrument" was built in software to "sample" the model results. This instrument was constructed assuming sample blank and calibration errors were independent and that each was randomly encountered. It was assumed that each error term was normally distributed with mean 0 and variance equal to the precision and accuracy given above. A random number generator (randn, MatLab, MathWorks Inc., Natick, Massachusetts) whose product elements are normally distributed with mean 0 and variance 1 was used to supply a sample error probability factor which was multiplied by the actual instrument variance and that product was then added or subtracted from a model result. The results from this statistical CH_2O instrument are presented in the right-middle column of Figure 4 labeled "Sampled Model." The measured and sampled model observations are in much better agreement although measured distributions remain broader. This suggests random measurement error does play a significant role in comparing measurements and model results at CH_2O levels observed during PEM-Tropics B. However, the difference in medians remains to be explained.

A south-to-north CH_2O transect from 38°S to 32°N and between 130° and 170°W longitude for the central Pacific is depicted in Figure 5. This includes a total of 3709 1-min merge product observations from ten P3-B flights on March 13, 1999, to April 9, 1999, and from twelve DC-8 flights on March 6, 1999, to April 13, 1999. The observations from both aircraft were pooled and stratified by latitude and altitude. Histograms are used to display the CH_2O observations as a function of latitude and altitude strata. As above the histogram cell width is 50 pptv, a cell bar height denotes number of occurrence, the leftmost cell (0-50 pptv) indicates LOD observations, the rightmost cell (550-600) represents all observations greater than 550 pptv, and the median value within a stratum is shown by the downward pointing triangle on each histogram. The nominal latitude of the Intertropical Convergence Zone (ITCZ) was at 7°N and the ITCZ and this latitude were used to anchor our latitudinal 10° stratification. The southernmost and northernmost strata are actually 15° in width in order to encompass observations over the full range of latitudes sampled. This expansion did not impact the distributions as shown, nor did it delete significant trends at the outer latitudinal limits. Altitude stratification was the same as in Figure 4. Stratum altitude range is given in the *Y* axis labels; latitude range is given across the top along with the zone number referenced to Figures 2a and c. Almost all observations above 8 km are from the DC-8. The latitude strata from 23°S to 17°N include multiple flights from both aircraft on multiple days. Sampled air masses at middle to low altitude were from all compass points, and the histograms are broad. It should be noted that the northernmost strata contains data from two flights, DC-8 flight 4 on March 6, 1999 (mainly zonal flow), and P3-B flight 18 on April 9, 1999 (flow principally from the north). The distributions below 4 km are broad and flat, reflecting this difference in air mass origin and small sample number. The southernmost strata contain data from DC-8 flights 14 and 18 on March 30, 1999, and April 9, 1999, respectively. The effect of limited flight numbers can be seen in the 0-1 km histogram for the 23°-38°S latitude zone. The histogram for this stratum was bimodal indicating two different air masses were sampled on the separate days. In flight 18 (April 10, 1999), backward trajectories suggest primarily a tropical origin for the air mass sampled; while in flight 14 (March 30, 1999), air mass backward trajectories imply a zonal to slightly polar air mass history. CH_2O was greater in the air with the more tropical trajectory.

A three-strata quasi west-to-east transect from 150°E to 230°W for latitudes between 3° and 23°S is shown in Figure 6. The leftmost column is for observations west of 170°W longitude and is composed of five DC-8 flights from March 17 to 26, 1999. The rightmost column shows data gathered east of 130°W on three DC-8 flights from April 13 to 17, 1999. The bulk of the data are in the central South Pacific region from seven DC-8 and six P3-B flights spanning the March 26 to April 13, 1999, time period. Histograms, defined identically as in Figures 4 and 5, are used to display the longitude-altitude variation in the observations. Below 4 km, median CH_2O for the central observational set is about 50-100 pptv greater than to either side. Above 6 km the central and western strata show median values between 50 and 100 pptv, whereas the eastern strata exhibit median values below the LOD. Meteorologically, the western region was influenced by the South Pacific Convergence Zone (SPCZ) and by a diffuse ITCZ, the central region was influenced by the eastern extension of the SPCZ, the ITCZ, and midlatitude cyclones, and the eastern region experienced fairer weather [*Fuelberg et al.*, this issue].

Continental pollutant plumes or layers were encountered on DC-8 flights 21 and 22 below 5 km. Ethylene, C_2H_4, propane, C_3H_8, CH_2O, and altitude are shown as a function of time for portions of each flight on Figure 7. The symbol spacing illustrates the resolution of the 1-min merge product. CH_2O and C_2H_4 mixing ratios below their LOD, 50 and 3 pptv, respectively, were assigned a value of zero for plotting purposes. On flight 21 a broad plume is noted between 2030 and 2130 UT. Plumes are also noted between 1800 and 1900 UT and between 2000 and 2030 UT on flight 22. All three events are below 5 km altitude with CH_2O maxima of 900, 1200, and 600 pptv at 1.8, 2.5, and 3.5 km for the three plumes, respectively. The maximum may not have been encountered on the last plume as the aircraft descended only to 3.5 km. Plume locations are qualitatively located on Figure 2a and labeled d21 and d22. It is interesting to note CH_2O increases in general with both hydrocarbons shown and the sharp peaks seen in CH_2O for the first plume of flight 22 correspond only with the sharp peaks in ethylene. All three plumes contained significantly elevated levels of hydrogen peroxide and CO, modestly elevated ozone and methylhydroperoxide, and little in the way of elevated NO. At the lowest altitudes during flights d21 and d22, *Blake et al.* [this issue] call out a strong urban continental influence as indicated by elevated levels of many urban trace gases, for example, C_2Cl_4, HCFC-141B, CH_2Cl_2, CH_4, C_3H_8, as well as short-lived n-C_6H_{14} and by air mass trajectories going back to Central and North America. The marine tracers dimethylsulfide, methyliodide, and bromoform were also elevated as might be expected below 1 km. Blake et al. noted the plumes between 1 and 5 km were very different in character. Here the air was highly stratified, with the plume layers containing the elevated CH_2O also particularly high in burning signature gases, such as C_2H_4, CO, C_2H_2, C_6H_6, and CH_3Cl. However, levels of the urban tracers, including propane, were lower than in the 0-1 km layer. The trajectories are complicated for these 1-5 km air masses, as

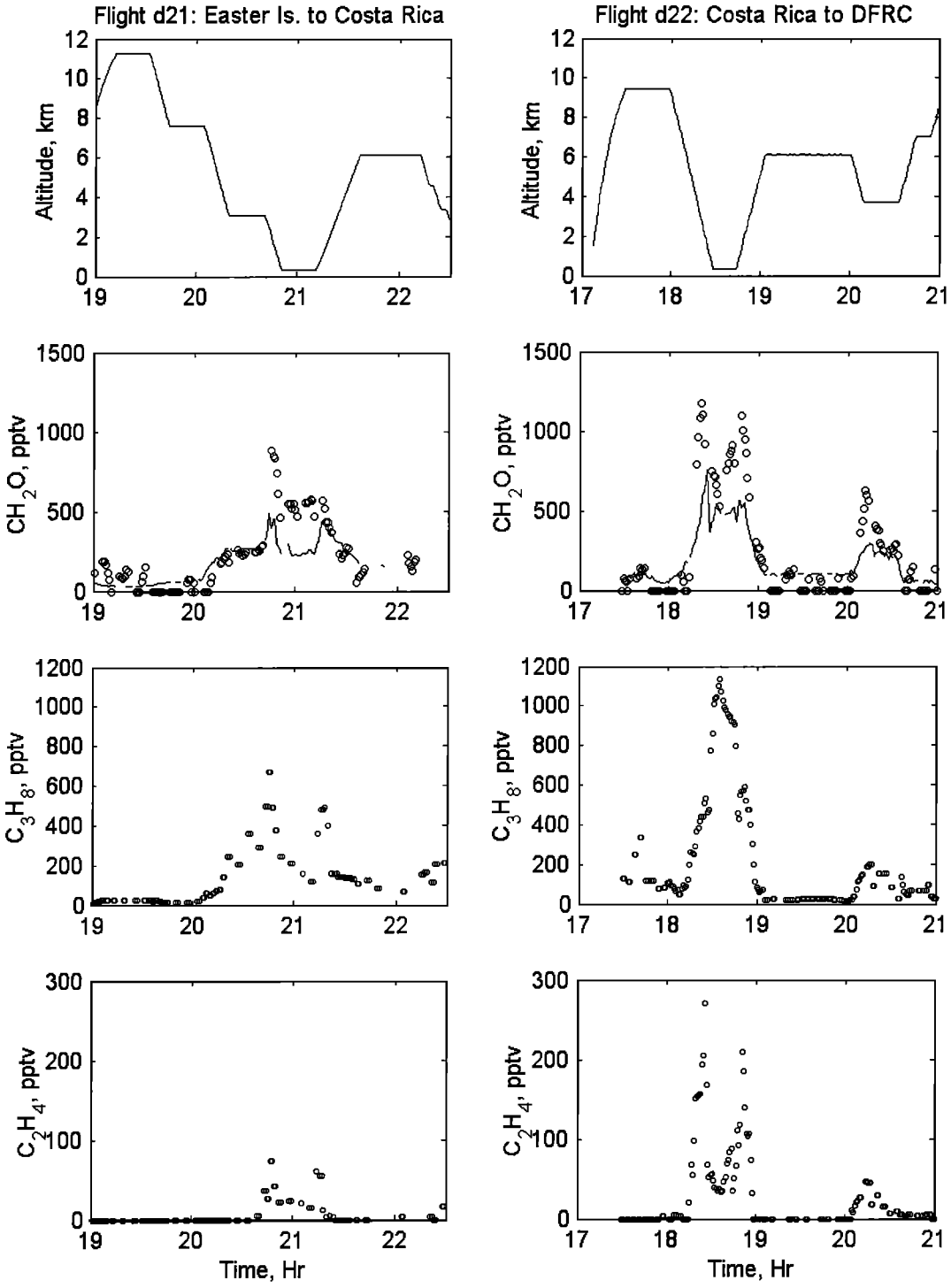

Figure 7. Time series for portions of DC-8 flights 21 (Easter Island to Costa Rica) and 22 (Costa Rica to NASA Dryden Flight Research Center) showing altitude (km), CH_2O (pptv), propane (pptv), and ethene (pptv). A plume or polluted layer in flight 21 is noted near 2100 UT. Plumes or generally polluted layers are noted at 1830 and 2020 UT in flight 22. The thin solid lines in the CH_2O panels show point model results.

they loop about over Central and North America and over northern regions of South America where biomass burning was likely.

In Figure 7 CH_2O the thin solid lines show model results. Model CH_2O showed a notable increase with hydrocarbons (e.g., ethane, propane, ethane), and spike with alkenes as did the measurements.

4. Discussion

The results shown above reinforce the prior observed and expected decrease in CH_2O with increasing altitude through the remote troposphere. This decrease is caused, in part, by the decrease in water vapor, HO, alkenes and other reactive hydrocarbons, and the consequent decrease in CH_2O sources

with altitude, while the CH_2O loss by photolysis increases with altitude [e.g., *Wang et al.*, this issue; *Logan et al.*, 1981; R.E. Shetter et al., manuscript in preparation, 2001]. *Arlander et al.* [1995] showed CH_2O decreased with altitude in the TROPOZ II flights circumnavigating the North Atlantic and South America in January-February, 1991. *Heikes et al.* [1996b] and *Lee et al.* [1998] demonstrated this in TRACE-A over the South Atlantic (September-October, 1992), and this was also noted over the North Atlantic in October-November, 1997, for SONEX (unpublished results) and in September 1997, during NARE 1997 (A. Fried et al., manuscript in preparation, 2001). The CH_2O mixing ratios observed in PEM-Tropics B are comparable to those observed during TROPOZ II for all altitudes within the overlapping latitude regime after segregating out their data thought to be influenced by pollution or near land surface emissions. TROPOZ II observations show a decrease from about 500 pptv at 3 km to 50 pptv at 10 km, whereas the data shown here decrease from about 250 pptv at 3 km to 50 pptv by 10 km. At times, Arlander et al.'s TROPOZ II measurements were influenced by the continents, and under comparable polluted conditions we observed similar mixing ratios (600-1200 pptv) and plume heights (peaks between 1 and 4 km) on DC-8 flights 21 and 22 over the ocean near Central America and the west coast of South America. In contrast, the TRACE-A South Atlantic CH_2O data for continental outflow cases [*Talbot et al.*, 1996] correspond well with the unpolluted South American coastal TROPOZ II data and the PEM-Tropics B data, but Talbot et al.'s TRACE-A data for the aged marine case are lower than those reported here or in TROPOZ II.

Near Hawaii, 17°-32°N in Figure 5, the 2-6 km and the 0-2 km CH_2O mixing ratios are comparable to those shown for free troposphere and upslope air, respectively, by *Heikes et al.* [1996a] and *Zhou et al.* [1996] for the Mauna Loa Observatory Photochemistry Experiment (MLOPEX) 2c at Mauna Loa Observatory, Hawaii, in March-April, 1992. Our 0-2 km values are comparable to upslope conditions during MLOPEX 1 in April-June, 1988, but our 2-6 km values are greater than those determined for free tropospheric air in MLOPEX 1 [*Heikes*, 1992]. Upslope air at Mauna Loa is composed of marine boundary layer air masses as modified by island emissions and can be compared with the 0-2 km measurements. Downslope or free tropospheric air at Mauna Loa consists of air masses from the lower middle troposphere and are relatively free of island emissions and can be compared with measurements from 2-6 km.

Comparisons can be made between marine boundary layer measurements. *Weller et al.* [2000] report shipboard measurements from the Atlantic, which show a latitudinal gradient from the equator (nominally 1000 pptv) to 35°S (nominally 300 pptv) with three episodes below 200 pptv. Our low-altitude observations for the central Pacific are at the mid to low end of theirs for the South Atlantic. *Arlander et al.* [1990] reported shipboard measurements of CH_2O from the Soviet American Gas and Aerosol Experiment (SAGA) 2 cruise (April-July, 1987). Leg 1 of this cruise in May-June 1987 was a north-to-south transect across the western Pacific and went from the Kamchatka Peninsula, Siberia, to New Zealand approximately along 165°E. On this leg, CH_2O averages (5° latitude averages) ranged between 400 and 800 pptv north of 5°S. South of 30°S their means ranged from 100 to 200 pptv. From 30°S to 5°S, mean CH_2O increased from 100 to 400 pptv. Figure 5 shows our composite north-to-south transect across the central Pacific from 38°S to 32°N in which our 0-1 km median values for CH_2O vary from 200 to 400 pptv. Leg 3 of the SAGA 2 cruise in June-July 1987 was a west-to-east transect along 5°N from Malaysia to the Dateline. Mean (5° longitude averages) CH_2O values varied from 700 to 1200 pptv until near 170°E where they decreased to about 650 pptv. Our near-surface data (Figures 5 and 6) rarely exceeded 550 pptv and the near-surface median values in the tropics and subtropics were all between 300 and 400 pptv. The PEM-Tropics B CH_2O marine boundary layer observations were consistently less than those of SAGA 2 north of 23°S..

South of Australia (south of 30°S from 95°E to 170°E) on SAGA 2 leg 2, *Arlander et al.* [1990] reported surface CH_2O means between 50 and 200 pptv as compared to legs 1 and 3 where mean values were between 400 and 1200 pptv. We have limited observational data to compare with leg 2 as there were only two flights flown south of 23°S. On one the near-surface CH_2O mode was 175, and on the other it was 300 pptv (see Figure 5 stratum for 23°-38°S and 0-1 km). *Ayers et al.* [1997] reported marine boundary layer CH_2O mixing ratios between 250 and 450 pptv for Cape Grim, Tasmania (43°S), during November-December 1992. These mixing ratios are comparable or slightly higher than the southernmost marine boundary layer mixing ratios reported here.

A note of caution is warranted with respect to the marine boundary layer CH_2O data. *Gilpin et al.* [1997, and references therein] summarized several studies and a recent CH_2O techniques intercomparison that demonstrated DNPH-coated C-18 and silica gel cartridge methods were subject to positive interferences from O_3 and other gases. *Arlander et al.* [1990; 1995] used such a method. Thus artificially high values could have been reported by them although such an interference is expected to be small because of the low O_3 and alkene concentrations encountered in the marine boundary layer. Also, a comparison of their technique with a diffusion scrubber fluorescence technique was quite good [*Trapp and de Serves*, 1995]. The diffusion scrubber method was used by *Ayers et al.* [1997] at Cape Grim and was examined in the Gilpin et al. study. It was shown to yield measurements consistent with the other methods tested. The *Lazrus et al.* [1988] method used here was also a part of the Gilpin et al. study and found to yield valid measurements once a calibration issue had been resolved. Whether the above noted differences in reported marine boundary layer CH_2O are the result of geographical, seasonal, interannual, altitude (the DC-8 did not sample below 0.3 km nor did the P3-B sample below 0.05 km), or instrumental differences is indeterminate.

The comparison is good between point model result and measurement medians as shown for example, in Figure 4 (comparisons for other latitude-longitude-altitude strata are similar and not shown), although the measurements are consistently and significantly higher. A point-by-point comparison of measurements and model results is poor with considerable variability possibly introduced by measurement precision and other natural factors such as convective transport and cloud radiation effects. The correlation between observed and modeled CH_2O was significant for the entire data set (not shown), but this was primarily forced by the plume events noted earlier near Central America and a few other observations near islands. J. Snow et al. (unpublished manuscript, 2001) noted a trend in CH_2O with hydrocarbons

when comparing and contrasting convectively influenced air masses with the background free troposphere. Their analysis indicated that CH_2O tracked the convective tracers, as did hydrocarbons, with the exception of one case in which the background air contained high hydrocarbon levels and higher CH_2O mixing ratios. It was inferred that parent hydrocarbon concentrations were as or more important than vertical transport in establishing CH_2O levels.

Near-surface CH_2O was approximately 150 pptv higher than modeled (e.g., Figure 4). PEM-Tropics B was conducted in the wet season for this area with convection and precipitation events noted on most flights. To account for surface deposition and precipitation removal effects, the point model adds in an additional fixed rate of loss for CH_2O below 1 km. This "deposition" loss rate was set equal to 1.3×10^{-5} s^{-1} which is approximately ¼ that of the CH_2O photochemical loss rate. It is conceivable this rate was overestimated in the model. Ignoring physical removal completely in the model would make the model results higher by as much as 20% or about 35 pptv but still leaves a bias. The model also uses observed photolysis rates to set a 24-hour cloud-impacted photolysis rate. Variability in photolysis rates are estimated, on the basis of clear-to-cloudy sky conditions, to add at most another 10% to the variability in modeled CH_2O. However, this is not expected to impact the mean difference. In addition, precipitation and surface removal are episodic events that would introduce variability in the observations that is not captured in the model [*Thompson and Cicerone*, 1982]. These processes would further degrade model-measurement correlation in the lower altitudes as was noted above.

Other sources of CH_2O, not explicitly carried in the point model but potentially active in the boundary layer and throughout the troposphere, were considered in explaining the bias between point model results and the observations. Methanol was observed throughout the troposphere [*Singh et al.*, 2001]. On many flights, dimethylsulfide (DMS), bromoform, and methylnitrate correlated with CH_2O when descending and ascending into and out of the marine boundary layer. Median boundary layer DMS was nominally 120 pptv (D. Thornton et al., manuscript in preparation, 2001), and assuming its oxidation yields two CH_2O molecules as an upper limit, it would add approximately 18 pptv of CH_2O to that already calculated. Median boundary layer methanol and ethanol were 947 and 50 pptv [*Singh et al.*, 2001], and their inclusion in the model would add approximately 17 pptv of CH_2O. Higher-order alkenes, for example, propene, were individually near and below their respective LOD's [*Blake et al.*, this issue]. Using an assumed value of 10 pptv in the model to account for the sum of all possible alkenes, the inclusion of alkenes would add an additional 5 pptv of CH_2O. Together, the inclusion of these species adds only 40 pptv of CH_2O, which is insufficient to close the measurement-model gap.

Precipitation and convection are natural processes occurring in the study area wet season and which would act to increase CH_2O variability. *Singh et al.* [2001] compared observed CH_2O with the results from a three-dimensional photochemical transport model. This analysis used spatial-height averaged data for comparison with model results and showed excellent agreement in the aggregate for all altitudes. *Wang et al.* [this issue] and *Ravetta et al.* [this issue] have illustrated measurement-model result differences at higher altitudes, too. Wang et al. using average concentrations for several photochemically active species to constrain their model's chemistry and transport, initially underpredicted CH_2O at high altitude. They were able to reconcile a large part of the difference in their one-dimensional vertical diffusion model by including a more rapid diffusive transport parameterization and by inclusion of data below LOD. The more rapid vertical mixing was indicated by model-measurement comparison of other tracers (e.g., methyliodide). This transport effectively moved CH_2O from lower altitudes to higher ones. On DC-8 flight 15, sampling at one altitude repeatedly sampled two air masses, one which was strongly influenced by the recent upward transport of air from below and one which was considered to be little impacted by recent vertical motion. Ravetta et al. showed the recent convectively influenced air mass CH_2O mixing ratio was 170 pptv as compared to 120 pptv for the nonconvectively influenced air. The Wang et al. and Ravetta et al. works illustrate the effect vertical motion would have on increasing ambient CH_2O variability.

The point model results are very much smaller than the *Arlander et al.* [1990] Pacific surface data set by a factor of 2-3 with the exception of SAGA 2 leg 2 (south of Australia and south of 30°S from 95°E to 170°E). Measured nonmethane hydrocarbon concentrations, for example, ethene, propene, were also much smaller in PEM-Tropics B [*Blake et al.*, this issue] than those reported by Arlander et al. *Ayers et al.* [1997] reported their observations were 50% higher than a standard point model would predict. In addition, *Weller et al.* [2000] for the South Atlantic marine boundary layer reported their CH_2O observations were a factor of 3 greater than point model results; although their three clean episodes noted above were closer in agreement with the point model. In contrast *Junkermann and Stockwell* [1999] showed agreement between their measurements and model simulations for the same South Atlantic region. Lastly, *Jacob et al.* [1996] and *Heikes et al.* [1996b] showed modeled values were significantly higher than measured marine boundary layer air in TRACE-A but that model and measured CH_2O mixing ratios agreed well in the free troposphere.

Singh et al. [2001] has shown that the total concentration of identified oxygenated carbon compounds observed in PEM-Tropics B is equal to or exceeds the total concentration of non-methane hydrocarbons. Several of these species are photochemically active, for example, acetone, acetaldehyde, methylhydroperoxide, formaldehyde, and others less so, for example, methanol, peroxyacetylnitrate, formic acid, acetic acid. CH_2O contributed between 5 and 10% of the total carbon in oxygenated carbon compounds over the central Pacific and ranked fourth behind methanol, methylhydroperoxide, and acetone. Collectively, since oxygenate chemistry is less well known than that of the other nonmethane hydrocarbons, oxygenates may play a greater role in the atmospheric carbon cycle and CH_2O chemistry than previously thought. Large differences existed in the comparison of measured acetone and acetaldehyde to their model results [*Singh et al*, 2001]. These differences and those noted in CH_2O here may well be linked and the result of inadequate consideration of oxygenates chemistry.

The higher than modeled CH_2O mixing ratios observed at high altitude in PEM-Tropics B represent a significant source of HO_x [*Wang et al.*, this issue; *Ravetta et al.*, this issue; J.M. Rodriquez et al., manuscript in preparation, 2001], the importance of which remains to be established. Ravetta et al.,

in their analysis of the DC-8 flight 15 convective event, state the inclusion of measured CH_2O mixing ratios in their model gave rise to significantly more HO_x than when their model-derived CH_2O was used but that these high HO_x levels exceeded those observed. *Crawford et al.* [1999] in an analysis of upper tropospheric HO_x showed model HO_x to be most sensitive to CH_2O in the upper troposphere.

Closure between measured HO_x precursors, modeled HO_x production rates, and measured HO_x species was not fully achieved and CH_2O is one link in these processes requiring improved understanding. How well the chemistry of CH_2O is understood in the remote atmosphere remains an open question [e.g., *Arlander et al.*, 1995; *Jacob et al.*, 1996; *Ayers et al.*, 1997; *Junkermann and Stockwell*, 1999; *Jaegle et al.*, 2000; *Weller et al.*, 2000; G.J. Frost et al., manuscript in preparation, 2001]. There is confidence in the photochemical mechanisms employed, especially in the remote regions where CH_4 chemistry is expected to dominate. Yet, the role of oxygenates [e.g., *Singh et al.*, 2001] and a few mechanistic details [e.g., *Ayers et al.*, 1997; *Ravetta et al.*, this issue] remain to be determined. There is equal confidence in the measurements as systematic factors, interferences, or artifacts are not thought to compromise the measurement methods [*Kleindienst et al.*, 1988; *Lawson et al.*, 1990; *Trapp and de Serves*, 1995; *Heikes et al.*, 1996a; *Gilpin, et al.*, 1997; *Ayers et al.*, 1997; *Weller et al.*, 2000]. However, these intercomparisons were all performed over land with ambient levels well in excess of a few hundred pptv, and an intercomparison in the remote marine conditions remains to be performed.

5. Conclusion

CH_2O mixing ratios were presented from the 22 DC-8 flights and the 19 P3-B flights, which comprised the NASA GTE PEM-Tropics B mission. This experiment took place during a 2-month period, March-April 1999, and was flown over the tropical and subtropical Pacific extending from the surface to 12 km altitude. Median CH_2O was observed to decrease from nominally 300 pptv at the surface to 75 at 6 km and to near 50 pptv above 10 km. Between 23°S and 32°N and above 1 km, median CH_2O mixing ratios were nearly constant with latitude over the central Pacific: nominally, 200 pptv 2-4 km, 75 pptv 6-8 km, and 50 pptv 10-12 km. Between 3° and 23°S, median CH_2O mixing ratios were lower in the eastern tropical Pacific than in the western or central Pacific; nominal differences were >100 pptv near the surface to ~100 pptv at midaltitude to ~50 pptv at high altitude. Along the coast of Central America and Mexico between 1 and 4 km altitude, off-continent plumes were encountered in which CH_2O mixing ratios exceed 800 pptv and went as high as 1200 pptv. CH_2O was correlated with hydrocarbons but this was driven primarily by plume events. Spatial averaged measurements were in good agreement with similarly averaged point, one-dimensional and three-dimensional model results, whereas individual point-by-point model-measurement comparison was poor. Measurement variance induced by instrumental effects and natural variability, possibly from convection and precipitation events, obscured point-by-point analysis of the data.

Acknowledgments. This work was supported in part by NASA grants NCC-1-302, MIPR L69496D, NCC 1-306, and NCC-1-299 to B.H., D.O., D.D. and D.B., respectively. Priscilla Burrows is thanked for her efforts during the field phase of the mission. Thanks are also given to the reviewers for their critical effort in improving the manuscript.

References

Arlander, D.W., D.R. Cronn, J.C. Farmer, F.A. Menzia, and H.H. Westberg, Gaseous oxygenated hydrocarbons in the remote marine troposphere, *J. Geophys. Res., 95*, 16,391-16,403, 1990.

Arlander, D.W., D. Bruning, U. Schmidt, and D.H. Ehhalt, The tropospheric distribution of formaldehyde during TROPOZ II, *J. Atmos. Chem., 22*, 251-268, 1995.

Avery, M., et al., Chemical transport across the ITCZ in the central Pacific during an ENSO cold phase event in March/April of 1999, *J. Geophys. Res.*, this issue.

Ayers, G.P., R.W. Gillett, H. Granek, C. de Serves, and R.A. Cox, Formaldehyde production in clean marine air, *Geophys. Res. Lett., 24*, 401-404, 1997.

Blake, N.J., et al., Large-scale latitudinal and vertical distributions of NMHCs and selected halocarbons in the troposphere over the Pacific Ocean during the March-April 1999 Pacific Exploratory Mission (PEM-Tropics B), *J. Geophys. Res.*, this issue.

Browell, E.V., et al., Large-scale air mass characteristics observed over the remote tropical Pacific Ocean during March-April 1999: Results from PEM-Tropics B field experiment, *J. Geophys. Res.*, this issue.

Chameides, W.L., and D.D. Davis, Aqueous phase source of formic acid in clouds, *Nature, 304*, 427-429, 1983.

Cohan, D.S., M.G. Schultz, D.J. Jacob, B.G. Heikes, and D.R. Blake, Convective injection and photochemical decay of peroxides in the tropical upper troposphere: Methyl iodide as a tracer of marine convection, *J. Geophys. Res., 104*, 5717-5724, 1999.

Crawford, J., et al., Assessment of upper tropospheric HO_x sources over the tropical Pacific based on NASA GTE/PEM data: Net effect on HO_x and other photochemical parameters, *J. Geophys. Res., 104*, 16,255-16,273, 1999.

Finlayson-Pitts, B.J., and J. N. Pitts Jr., *Atmospheric Chemistry: Fundamentals and Experimental Techniques*, John Wiley, New York, 1986.

Fuelberg, H., et al., A meteorological overview of the second PEM-Tropics, this issue.

Gilpin, T., et al., Intercomparison of six ambient [CH_2O] measurement techniques, *J. Geophys. Res., 102*, 21,161-21,188, 1997.

Heikes, B.G., Formaldehyde and hydroperoxides at Mauna Loa Observatory, *J. Geophys. Res., 97*, 18,001-18,013, 1992.

Heikes, B.G., et al., Formaldehyde methods comparison in the remote lower troposphere during the Mauna Loa Observatory Photochemistry Experiment 2, *J. Geophys. Res., 101*, 14,741-14,755, 1996a.

Heikes, B.G., M. Lee, D.J. Jacob, R. Talbot, H. Singh, D. Blake, B. Anderson, H. Fuelberg, and A.M. Thompson, Ozone, hydroperoxides, oxide of nitrogen, and hydrocarbon budgets in the marine boundary layer over the South Atlantic., *J. Geophys. Res., 101*, 24,221-24,234, 1996b.

Hoell, J.M., D.D. Davis, D.J. Jacob, M.O. Rogers, R.E. Newell, H.E. Fuelberg, R.J. McNeal, J.L. Raper, and R.J. Bendura, Pacific Exploratory Mission in the tropical Pacific: PEM-Tropics A, August-September 1996, *J. Geophys. Res., 104*, 5567-5583, 1999.

Jacob, D.J., Chemistry of HO in remote clouds and its role in the production of formic acid and peroxymonosulfate, *J. Geophys. Res., 91*, 9807-9826, 1986.

Jacob, D.J., et al., Origin of ozone and NO_x in the tropical troposphere: A photochemical analysis of aircraft observations over the South Atlantic Basin, *J. Geophys. Res., 101*, 24,235-24,250, 1996.

Jaegle, L., et al., Observed OH and HO_2 in the upper troposphere suggest a major source from convective injection of peroxides, *Geophys. Res. Lett., 24*, 3181-3184, 1997.

Jaegle, L., et al., Photochemistry of HO_x in the upper troposphere at northern midlatitudes, *J. Geophys. Res., 105*, 3877-3892, 2000.

Junkermann, W., and W. R. Stockwell, On the budget of photooxidants in the marine boundary layer of the tropical South Atlantic, *J. Geophys. Res., 104*, 8039-8046, 1999.

Kleindienst, T.E., et al., An intercomparison of formaldehyde measurement techniques at ambient concentrations, *Atmos. Environ., 22*, 1931-1939, 1988.

Lawson, D.R., H.W. Biermann, E.C. Tuazon, A.M. Winer, G.I. Mackay, H.I. Schiff, G.L. Kok, P.K. Dasgupta, and K. Fung, Formaldehyde measurement methods evaluation and ambient concentrations during the carbonaceous species methods comparison study, *Aerosol Sci. Technol., 12*, 64-67, 1990.

Lazrus, A., K. Fong, and J. Lind, Automated fluorometric determination of formaldehyde in air, *Anat. Chem., 60*, 1074-1078, 1988.

Lee M., B.G. Heikes, D.J. Jacob, G. Sachse, and B. Anderson, Hydrogen peroxide, organic peroxides, and formaldehyde as primary pollutants from biomass burning, *J. Geophys. Res., 102*, 1301-1309, 1997.

Lee., M., B.G. Heikes, and D.J. Jacob, Enhancements of hydroperoxides and formaldehyde in biomass burning impacted air and their effect on atmospheric oxidant cycles, *J. Geophys. Res., 103*, 13,201-13,212, 1998.

Lee, Y-N., and X. Zhou, Method for the determination of some soluble atmospheric carbonyl compounds, *Environ. Sci. Technol., 27*, 749-756, 1993.

Logan, J.A., M.J. Prather, S.C. Wofsy, and M.B. McElroy, Tropospheric chemistry: A global perspective, *J. Geophys. Res., 86*, 7210-7254, 1981.

Olson, J., et al., Seasonal differences in the photochemistry of the South Pacific: A comparison of observations and model results from PEM-Tropics A and B, *J. Geophys. Res.*, this issue.

Prather, M.J., and D.J. Jacob, A persistent imbalance in HO_x and NO_x over the tropical South Pacific, *Geophys. Res. Lett., 24*, 3189-3192, 1997.

Raper, J.L., M.M. Kleb, D.J. Jacob, D.D. Davis, R.E. Newell, H.E. Fuelberg, R.J. Bendura, J.M. Hoell, and R.J. McNeal, Pacific Exploratory Mission in the tropical Pacific: PEM-Tropics B, March-April 1999, *J. Geophys. Res.*, this issue.

Ravetta, F., et al., Experimental evidence for the importance of convected methylhydroperoxide as a source of hydrogen oxide (HO_x) radicals in the tropical upper troposphere, *J. Geophys. Res.*, this issue.

Singh, H.B., M. Kanakidou, P.J. Crutzen, and D.J. Jacob, High concentrations and photochemical fate of oxygenated hydrocarbons in the global troposphere, *Nature, 378*, 50-54, 1995.

Singh, H., et al., Distribution and fate of selected oxygenated organic species in the troposphere and lower stratosphere over the Atlantic, *J. Geophys. Res., 105*, 3795-3805, 2000.

Singh, H., Y. Chen, A. Staudt, D. Jacob, D. Blake, B. Heikes, and J. Snow, Dominant presence of oxygented organic species in the remote troposphere, *Nature, 410*, 1078-1081, 2001.

Stockwell, W.R., and J.G. Calvert, The mechanism of NO_3 and HONO formation in the nighttime chemistry of the urban atmosphere, *J. Geophys. Res., 88*, 6673-6682, 1983.

Sumner, A., and P. Shepson, Influence of snowpack on formaldehyde in the Arctic troposphere (abstract), *Eos Trans. AGU, 79*(45), Fall Meet. Suppl., 94, 1998.

Talbot, R.W., et al., Chemical characteristics of continental outflow over the tropical South Atlantic Ocean from Brazil and Africa, *J. Geophys. Res., 101*, 24,187-24,202, 1996.

Thompson, A.M., and R.J. Cicerone, Clouds and wet removal as causes of variability in the trace-gas composition of the marine troposphere, *J. Geophys. Res., 87*, 8811-8826, 1982.

Thompson, A.M., and O. Zafiriou, Air-sea fluxes of transient atmospheric species, *J. Geophys. Res., 88*, 6696-6708, 1983.

Trapp, D., and C. de Serves, Intercomparison of formaldehyde measurements in the tropical atmosphere, *Atmos. Environ, 29*, 3239-3243, 1995.

Wang, Y., et al., Factors controlling the tropospheric O_3, OH, NO_x and SO_2 over the tropical Pacific during PEM-Tropics B, *J. Geophys. Res.*, this issue.

Weller, R., A. Boddenberg, S. Gab, O. Schrems, and G. Gautrois, Meridional distributions of hydroperoxides and formaldehyde in the marine boundary layer of the Atlantic (48°N- 35°S) measured during the Albatross campaign, *J. Geophys. Res., 105*, 14,401-14,412, 2000.

Wennberg, P.O., et al., Hydrogen radicals, and the production of O_3 in the upper troposphere, *Science, 279*, 49-53, 1998.

Zhou, X., and K. Mopper, Carbonyl compounds in the lower marine troposphere over the Carribbean Sea and Bahamas., *J. Geophys. Res., 98*, 2385-2392, 1993.

Zhou, X., Y.-N. Lee, L. Newman, X. Chen, and K. Mopper, Tropospheric formaldehyde concentration at the Mauna Loa Observatory during the Mauna Loa Observatory Photochemistry Experiment 2, *J. Geophys. Res., 101*, 14,711-14,719, 1996.

P. Egli, B. Heikes (corresponding author), and J. Snow, Center for Atmospheric Chemistry Studies, Graduate School of Oceanography, University of Rhode Island, Narragansett, RI, 02882-1197. (zagar@notos.gso.uri.edu)

D. O'Sullivan, Department of Chemistry, United States Naval Academy, Annapolis, MD, 21402.

J. Crawford and J. Olson, Atmospheric Sciences Division, NASA Langley Research Center, Hampton, VA, 23681-2199.

G. Chen and D. Davis, School of Earth and Atmospheric Sciences, Georgia Institute of Technology, Atlanta, GA, 30332.

D. Blake and N. Blake, Department of Chemistry, University of California, Irvine, CA, 92717.

(Received October 6, 2000; revised January 8, 2001;
accepted January 9, 2001.)